Radiation Measurements 176 (2024) 107209

Contents lists available at ScienceDirect

Radiation Measurements

journal homepage: www.elsevier.com/locate/radmeas

Investigation on thermally assisted optically stimulated luminescence signal in natural CaF_2

Luan Santos Lima, Nancy Kuniko Umisedo, Elisabeth Mateus Yoshimura *

Institute of Physics, Universidade de Sao Paulo, SP, Brazil

ARTICLE INFO

Keywords:
Natural fluorite
OSL
Thermally assisted OSL

ABSTRACT

In this work, thermally assisted OSL (TA-OSL) of natural fluorite was investigated, aiming to understand better the role of traps in both TL and OSL. TA-OSL is the luminescence simultaneously stimulated by light and heat; from this combination it is possible to access deeper traps in the analyzed material, that, in general, need more energy to be accessed. Irradiations were performed at room temperature using the Sr-90/Y-90 source incorporated in the TL/OSL reader at a dose rate of about 10 mGy/s. The optical stimulus was blue light at 470 nm. The dosimeters were also irradiated with X and gamma-rays of various energies (from 20 keV to 1.25 MeV) for comparing the energy dependence of the OSL and the TA-OSL signals. Residual TL curves were acquired after OSL readouts for checking trap participation in OSL emission. The OSL measurements were done at temperatures from 25 °C to 400 °C. For readout temperatures from 25 to ~185 °C, decay curves were observed, and they were modeled by one stretched-exponential function, giving rise to a good fit to the experimental data. The dependence of the fitting parameter (β) on the photon energy was studied, and it was observed that β increases with the X-ray beam effective energy. The energy dependence of OSL signal is 1.5 times larger than that of TA-OSL signal, pointing to the reduction in energy dependence with the combination of thermal and optical stimuli. The total light emitted (TA-OSL + residual TL) is highly increased by the simultaneous stimulation by light and heat, indicating that light promotes charges to thermally active traps (phototransfer), and heat promotes charges to optically active traps, facilitating their release during illumination.

1. Introduction

Natural calcium fluoride (fluorite, or fluorspar) is a mineral employed in various fields – from jewelry to hydrofluoric acid production. It exhibits a cubic face-centered lattice, with calcium ions at the corners and the face centers, with fluorine ions at the center of smaller cubes (side 1/8th of the unit cell) inside the unit cell [Topaksu et al., 2016]. This lattice structure can receive many impurities, such as, for instance, rare earths, which can affect the material luminescent properties, as reviewed by Sunta [1984]. Calcium fluoride is a known luminescent material, that has been used and studied as a thermoluminescent (TL) [Trowbridge and Burbank, 1898; Sunta, 1983] and optically stimulated luminescent (OSL) [Miller et al., 1988] material. Various compositions of CaF_2 crystals have been included in the list of available commercial TL and OSL materials [McKeever, 2022]. Topaksu and co-workers established that both a natural and a synthetic (TLD-400) CaF_2 samples display a TL glow curve that is commensurate with the presence of close overlapping groups of components, linked probably to a continuum distribution of trap levels [Topaksu et al., 2016]. The Brazilian fluorite that we studied here is in use as a personal TL dosimeter since long [Trzesniak et al., 1990] and has interesting OSL and TL properties [Ferreira et al., 2014]. In this paper we have observed Thermally Assisted Optically Stimulated Luminescence (TA-OSL) from natural Brazilian fluorite pellets at various temperatures. Performing the optical stimulation at higher temperatures results in an increase in the OSL efficiency, as the simultaneous thermal release of charge carriers provides various possibilities of charge retrapping and recombination, as well as the inactivation of shallow traps. Besides being dependent on the temperature, the intensity enhancement varies with the light stimulus wavelength, being more intense for low energy photons. The rate of decay of the CW-OSL signal is also temperature dependent [McKeever et al., 1997; McKeever, 2022; Spooner, 1994; Williams and Spooner, 2020]. The objective of this study is to understand better the OSL and TL mechanisms of this phosphor. The use of TA-OSL offers the possibility of interrogating defects that are not accessible by a thermal or luminous stimulus separately.

* Corresponding author.
E-mail address: yoshimura@usp.br (E.M. Yoshimura).

https://doi.org/10.1016/j.radmeas.2024.107209
Received 27 February 2024; Received in revised form 7 May 2024; Accepted 20 June 2024
Available online 21 June 2024

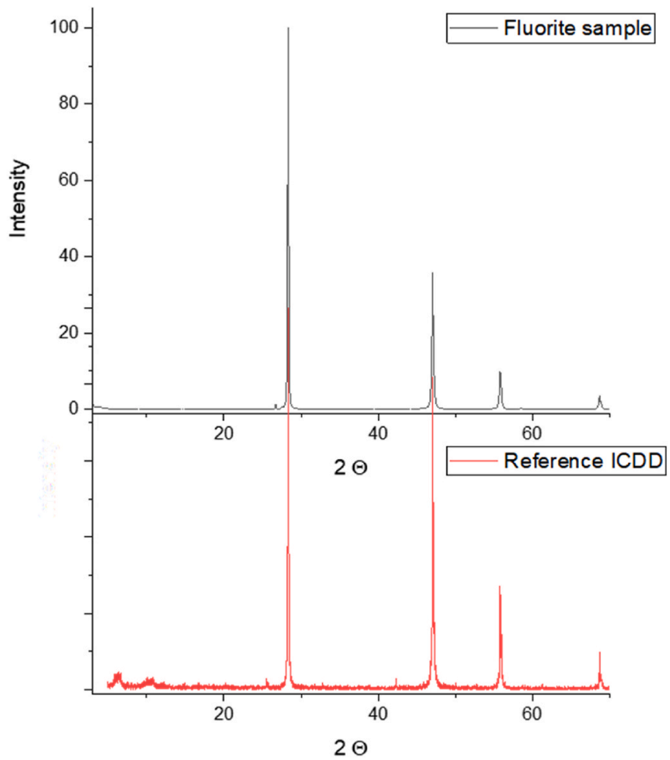

Fig. 1. X-ray diffraction pattern of a pellet used in this study. Compared to the ICDD reference.

2. Method and materials

Powdered green Brazilian fluorite previously treated at 600 °C per 15min was mixed with an inorganic binder (Durabond 950, Cotronics Corporation) at a weight proportion of 100/30 wt, and cold pressed to produce 54 mg pellets (5 mm diameter and 1 mm height). These pellets were already assayed, and no interference of the binder could be perceived in TL and OSL measurements [Umisedo et al., 2020]. The chemical analysis of fluorite shows the presence of rare earths and aluminum [Valerio et al., 1991]. Powdered natural fluorite crystals were examined by powder X-Ray Diffraction (XRD) with an EMPYREAN diffractometer, equipped with a CuK_α radiation source (1.541 Å), operating at 40 mA-45 kV, in a 2θ interval between 10° and 50°. The obtained diffractogram was compared with the ICDD (International Centre for Diffraction Data) and ICSD (Inorganic Crystal Structure Database) databases. The TL and OSL measurements were performed in a Risø equipment, DA-20, using a 7.5 mm pack of U340 filters. OSL was acquired at CW mode, blue stimulus (470 nm, 80 mW/cm^2). Samples were irradiated in the Risø equipment, at room temperature with a beta source (^{90}Sr/^{90}Y maximum beta energy 2.27 MeV, activity ~1.5GBq, giving rise to a dose rate of about 10 mGy/s at the sample position). Irradiations were also performed with X rays (Philips MG 540, constant potential, W anode, kVp from 60 to 200 kV and various combinations of added filtration) according to ISO narrow qualities ISO [ISO, 2020]. A cobalt-60 gamma-ray source was also used to irradiate the samples (activity 199,52 mCi in 2007, gamma energies 1.17 and 1.33 MeV, sealed source fixed inside a lead irradiator with a conical aperture). The range of doses for all types of irradiations was from 5 to 100 mGy. Irradiations were performed always at room temperature.

For TA-OSL experiments, the samples were beta irradiated at the TL/OSL reader (10 mGy) (or irradiated with X or gamma-ray photons), heated in dark at a constant rate until a desired T_S temperature, which was kept constant during 300s for acquiring the OSL signal at CW mode. Immediately after the TA-OSL measurement, the residual TL curve (R-TL) was also registered at a heating rate of 1 K/s, to 450 °C.

The OSL signals (I_{OSL}) were fitted with one stretched-exponential (SE) function (or Kohlrausch function), as indicated In Equation (1), where I_0 is the OSL intensity, τ is a time constant, β is the stretching parameter, and C is a constant to take the background reading into account. The stretching parameter is dimensionless, and its values are in the interval ($0< \beta < 1$) [Berberan-Santos et al., 2005]. The fittings were performed with a Matlab script using minimum squares methods and

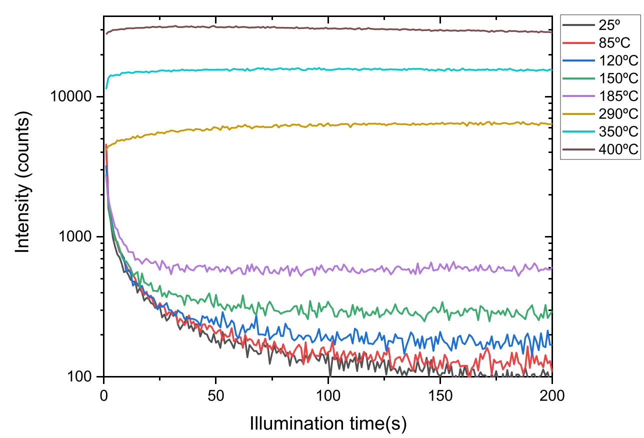

Fig. 3. TA-OSL of fluorite samples at various temperatures, after irradiation to 10 mGy.

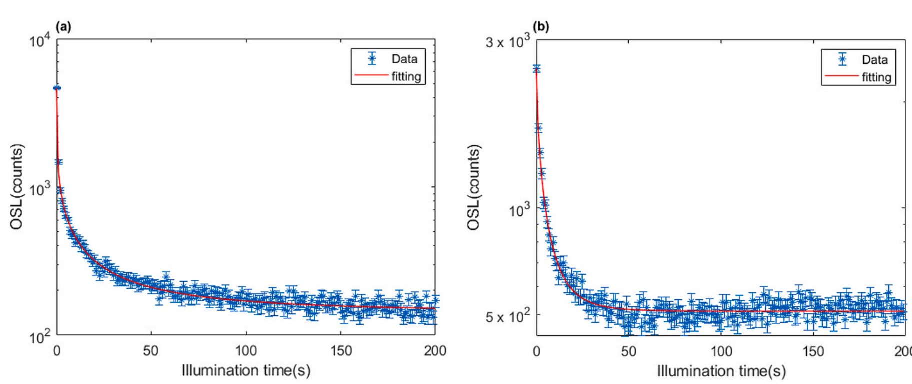

Fig. 2. Examples of the fitting of Equation (1) (red curves) to the OSL data (dots). (a) The OSL signal was acquired at room temperature, and the fitting parameters are: $I_0 = 4511 \pm 82$; $C = 143.3 \pm 1.7$; $\tau = 0.321 \pm 0.028$ s; $\beta = 0.309 \pm 0.007$; reduced chi-2 is 0.96, sample irradiated to 100 mGy. (b) TA-OSL acquired at 185 °C, with fitting parameters: $I_0 = 1976 \pm 58$; $\tau = 2.88 \pm 0.18$ s; $C = 511 \pm 2$; $\beta = 0.617 \pm 0.022$; reduced chi-2 is 0.97, sample irradiated to 10 m Gy.

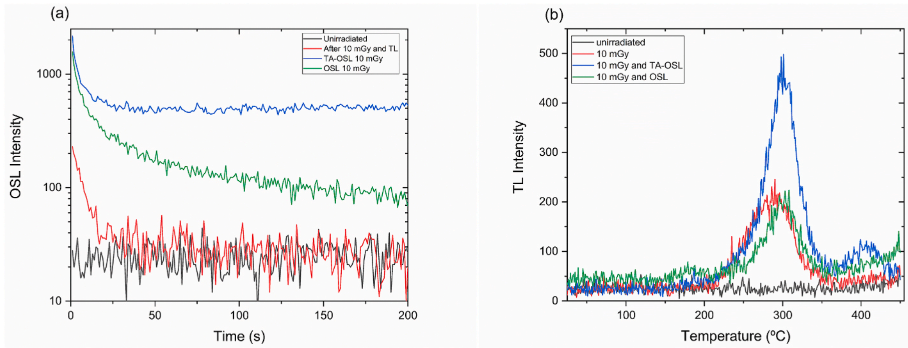

Fig. 4. (a) The OSL signals at room temperature of a non-irradiated (black line) and an irradiated (green line) sample. The blue signal is the TA-OSL at 185 °C, and the red signal corresponds to the same experiment, but with LEDs off. (b) The corresponding residual TL readouts after the acquisition of the signals shown in (a).

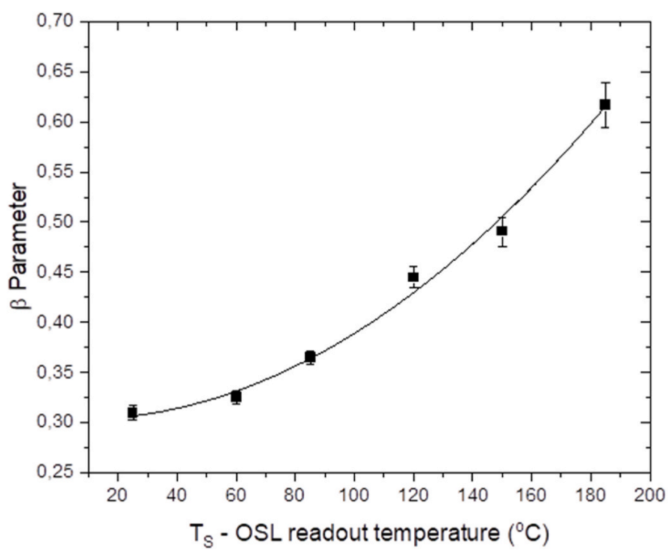

Fig. 5. Parameter β for TA-OSL curves fitted by Equation (1), at various T_S temperatures (data points). The solid curve is intended to guide the eyes.

calculating the respective reduced chi-2 for quality evaluation.

$$I_{OSL} = I_0 \exp\left(\frac{-t}{\tau}\right)^{\beta} + C \qquad \text{Equation (1)}$$

The SE functions is ubiquitous for describing relaxation phenomena, although it has been regarded as a convenient phenomenological tool without fundamental significance [Philips, 1996]. The rate equation obeyed by the SE functions has a time-dependent rate constant of the form $\lambda \propto t^{\beta-1}$, with $0 < \beta \leq 1$ [Plonka, 1986; Plonka et al., 1979]. The identification of the β parameter with the degree of disorder in the samples has focused the use of SE functions to explain relaxation phenomena on amorphous materials. In fact, Chen showed that this function likewise fits well the OSL decay of crystalline samples [Chen, 2003]. Chen and Leung hypothesized that β relates to the occurrence of high retrapping coefficients [Chen and Leung, 2003]. Later, Adamiec reported good fittings of SE function to experimental data obtained with multi-grain samples (quartz grains from Aeolian sediment), correlating the findings with sample heterogeneity, and reporting that SE fittings are equivalent to a sum of various exponential functions, with fewer parameters [Adamiec, 2005].

3. Results and discussion

3.1. Sample characterization

The X ray diffraction in Fig. 1 confirms the crystalline phases of calcium fluoride crystals, according to ICDD database. No other crystalline phases could be detected.

3.2. Optically stimulated luminescence

The CW-blue stimulated OSL acquired at room temperature, and the fitting with equation (1) for a 100 mGy beta irradiation is in Fig. 2 (a). In Fig. 2 (b) the fitting to TA-OSL at 185 °C (10 mGy) confirms that the SE fits well also the TA-OSL decay curve.

The T_S temperatures for TA-OSL were 85, 120, 150, 185, 290, 350 and 400 °C, and were chosen according to the known peak temperatures of the fluorite TL curve (~85, 180, and 290 °C), and of a 360 °C peak observed after optical bleaching [Ferreira et al., 2014]. Fig. 3 shows the observed TA-OSL curves, which present the expected decay aspect for the curves obtained with the four smaller temperatures (85, 120, 150 and 185 °C). For temperatures higher than those, the signal is almost

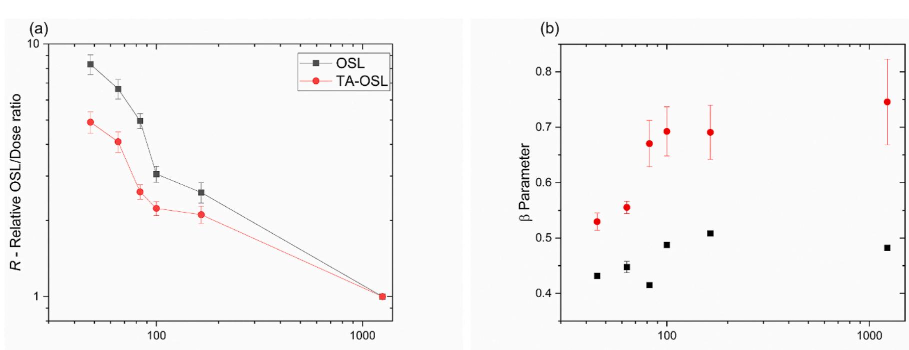

Fig. 6. (a) The energy response of OSL and TA-OSL signals (185 °C). For various X-ray beams, relative to the response to Co-60 gamma rays (the solid lines are guides for the eyes). (b) Variation of the β parameter for the same group of X-ray beams and both OSL signals.

constant for the whole interval of illumination and is more intense the higher is the T_S temperature. This behavior is consistent with thermally assisted photo-transfer already observed in the literature [Polymeris et al., 2006].

We focused on the 185 °C TA-OSL, as the signal is consistent with an OSL decay. Also, at this readout temperature, as the TL peak II vanishes, the role of the dosimetric peak (peak III at 290 °C) can be enhanced. To check for the isothermal emission contribution to the observed signal, a similar experiment, but with LED's off, was also performed. Fig. 4 (a) shows the illuminated and a non-illuminated TA-OSL signals, together with the room temperature OSL signal. Fig. 4 (b) shows the corresponding residual TL signals. It is interesting to notice that the residual dosimetric peak signal is more intense after a TA-OSL readout than after a room temperature OSL – almost a two-fold enhancement, indicating photo-transfer of charges to the dosimetric peak trap, as exhaustively studied by Chithambo [Chithambo, 2022]. A satellite peak at ∼400 °C appears in the R-TL signal after the TA-OSL readout. It is remarkable that the total light emission (OSL + R-TL) is highly increased by the simultaneous stimulation by light and heat, indicating that one or both processes occur: i) light promotes charges to thermally active traps that are posteriorly emptied by heat, ii) thermal activation (or phonon-coupling) promotes charges to optically active traps facilitating their release during illumination [McKeever, 2022]. Both the 185 °C TA-OSL and the corresponding R-TL net signals (after BG subtraction) have a linear response with dose (from 5 to 100 mGy) with a 0 intercept (results not shown here).

The TA-OSL curves (T_S temperatures till 185 °C) were also well fitted by the SE function (Equation (1)). The β parameter is higher for higher temperatures as shown in Fig. 5, consistent with an indication of augmented disorder. Although the interpretation of beta parameter is not a consensus in the literature, we highlight Adamiec's connection of the SE fitting with the presence of a multitude of independent grains in the sample, that might behave with some sort of individuality in OSL decay, because of their possible heterogeneity of origin [Adamiec, 2005]. As our samples do present grains from various fluorite polycrystals, this is a plausible hypothesis. Moreover, the proposition of the dosimetric trap having a continuum of energy levels [Topaksu et al., 2016] could be the explanation for the good quality fittings with SE functions, as this function can be interpreted as equivalent to a sum of simple exponential functions [Chen and Leung, 2003; Adamiec, 2005].

3.3. Energy response

The energy-response of the OSL and TA-OSL signals of the samples for X-rays and gamma radiation was investigated. It is expected that, at low photon energies, in a material like CaF_2, which has an effective atomic number much higher than that of air, the photon absorption process is more efficient, giving rise to a larger OSL signal. The dose response for room temperature OSL and TA-OSL for 185 °C was obtained for each X-ray and gamma-ray beam. For both signal types, linear responses were observed, with slopes (OSL/dose ratio) dependent on the photon energy. The energy dependence is usually shown by the variation of the ratio R – the relative OSL/dose ratio, defined in Equation (3), where the reference energy is the Co-60 gamma-ray energy.

$$R = \frac{\text{Slope of dose response at effective energy } E}{\text{Slope of dose response at the reference energy}} \qquad \text{Equation (3)}$$

Fig. 6 (a) shows a plot of R as a function of the effective energy of each photon beam. In Fig. 6 (a) it is possible to observe a change in the energy dependence of the dose response for TA-OSL (at 185 °C, red dots) compared to room temperature OSL (black dots): for TA-OSL the increase of the OSL response at low photon energies is smaller than it is for room temperature OSL. Complementing this outcome, the OSL decay curves obtained at 185 °C and at room temperature for pellets irradiated at each photon beam were fitted with Equation (1), to inspect if the curve shapes depend on photon energy. In fact, it was observed that the β parameter value increases with the photon energy of the irradiation beam for TA-OSL (Fig. 6 (b), red dots), but β does not change with the photon energy for the OSL curves obtained at room temperature (black dots in Fig. 6 (b)). A possible explanation for this behavior could probably be related to how photons lose energy in the material. The higher the photon energy the larger the mean distance travelled by secondary electrons in the material. Speculating, this could promote a larger disorder and phonon coupling with the energy transfer, resulting in larger β values, and smaller energy dependence.

4. Conclusions

The SE function was chosen to fit OSL signals of natural fluorite pellets, with good quality fittings. The same was observed for the TA-OSL of the same samples, for readout temperatures from 25 to 185 °C. SE function good fittings might be related to the existance of a continuum of energy levels for trapping the charge carriers, and to the presence of a multitude of grains which behave with some degree of heterogeneity when stimulated by light and heat. The parameter β showed an increase with the temperature used to perform the TA-OSL, which is commensurate with the association of β and disorder.

The fluorite pellets' emitted light (OSL and residual TL) is highly increased by the simultaneous stimulation by light and heat. This indicates that light promotes charges to thermally active traps that are subsequently emptied by heat, and, conversely, the thermal activation fosters charges to optically active traps facilitating their release during illumination. The charges released simultaneously with light and heat also populate a trap that gives rise to a TL peak observed at 405 °C in the residual TL signal.

According to our results, the energy dependence of the TA-OSL signal is lowered as compared to the room temperature OSL, and the shape of the decay curve changes with the photon energy, as the β parameter of the SE function increases with the effective energy of the beam. We speculate that these changes are connected to the mean distance travelled by secondary electrons in the material: it increases with photon energy and may promote larger disorder in the crystal, that manifests with higher stretching parameters in the OSL signal.

CRediT authorship contribution statement

Luan Santos Lima: Writing – original draft, Visualization, Software, Formal analysis, Data curation. **Nancy Kuniko Umisedo:** Resources, Methodology. **Elisabeth Mateus Yoshimura:** Writing – review & editing, Visualization, Supervision, Methodology, Investigation, Funding acquisition, Conceptualization.

Declaration of competing interest

The authors declare that they have no known competing financial interests or personal relationships that could have appeared to influence the work reported in this paper.

Elisabeth Mateus Yoshimura, on behalf of all authors.

Data availability

Data will be made available on request.

Acknowledgements

This work was supported by: Sao Paulo Research Foundation (FAPESP) [grant #2018/05982–0] and National Council for Scientific and Technological Development (CNPq) [grant #311657/2021–4].

References

Adamiec, G., 2005. OSL decay curves—relationship between single- and multiple-grain aliquots. Radiat. Meas. 39, 63–75. https://doi.org/10.1016/j.radmeas.2004.03.007.

Berberan-Santos, M.N., Bodunov, E.N., Valeur, B., 2005. Mathematical functions for the analysis of luminescence decays with underlying distributions 1. Kohlrausch decay function (stretched exponential). Chem. Phys. 315, 1–2. https://doi.org/10.1016/j.chemphys.2005.04.006, 171-182. ago.

Chen, R., 2003. Apparent stretched-exponential luminescence decay in crystalline solids. J. Lumin. 102–103, 510–518. https://doi.org/10.1016/S0022-2313(02)00601-4.

Chen, R., Leung, P.L., 2003. The decay of OSL signals as stretched-exponential functions. Radiat. Meas. 37, 519–526. https://doi.org/10.1016/S1350-4487(03)00007-6.

Chithambo, M.L., 2022. Phototransferred thermoluminescence of CaF_2: principles, analytical methods, and mechanisms. J. Appl. Phys. 132, 055102 https://doi.org/10.1063/5.0091205.

Ferreira, Jr F.A., et al., 2014. Correlation of optically and thermally stimulated luminescence of natural fluorite pellets. Radiat. Meas. 71, 254–257. https://doi.org/10.1016/j.radmeas.2014.02.020.

ISO, 2020. International Standards Organization -ISO – (ISO 4037-1) Radiological Protection — X and Gamma Reference Radiation for Calibrating Dosemeters and Doserate Meters and for Determining Their Response as a Function of Photon Energy — Part 1: Radiation Characteristics and Production Methods.

McKeever, S.W.S., 2022. A Course in Luminescence Measurements and Analyses for Radiation Dosimetry. Wiley.

McKeever, S.W.S.L., Botter-Jensen, L., Larsen, N.A., Duller, G.A.T., 1997. Temperature dependence of OSL decay curves: experimental and theoretical aspects. Radiat. Meas. 27, 161. https://doi.org/10.1016/S1350-4487(96)00106-0.

Miller, S.D., Endres, G.W.R., McDonald, J.C., Swinth, K.L., 1988. Cooled optically stimulated luminescence in CaF_2:Mn. Radiat. Protect. Dosim. 25, 201. https://doi.org/10.1093/oxfordjournals.rpd.a080372.

Philips, J.C., 1996. Stretched exponential relaxation in molecular and electronic glasses. Rep. Prog. Phys. 59 1133, 1996.

Plonka, A., 1986. Time-dependent reactivity of species in condensed media. In: Chemistry, V.40, Berthier, G., Dewar, M.J.S., Fischer, H., Fukui, K., Hall, G.G., Hartmann, H., Jaffe, H.H., Jortner, J., Kutzelnigg, W., Ruedenberg, K., Tomasi, J. (Eds.), Lecture Notes. Springer-Verlag Berlin Heidelberg, New York London Paris Tokyo.

Plonka, A., Kroh, J., Lefik, W., Bogus, W., 1979. Kinetics of trap-limited hydrogen atom decay in T-irradiated sulfuric acid glasses. J Phys Chern 83, 1807–1810.

Polymeris, G.S., Kitis, G., Tsirliganis, N.C., 2006. Correlation between TL and OSL properties of CaF_2:N. Nucl. Instrum. Methods Phys. Res. B 251, 133–142. https://doi.org/10.1016/j.nimb.2006.05.023.

Spooner, N.A., 1994. On the optical dating signal from quartz. Radiat. Meas. 23, 593.

Sunta, C.M., 1983. Irradiation effects on Ce^{3+} thermoluminescence centres of mineral CaF_2. Radiat. Eff. 79 (1–4), 149–158. https://doi.org/10.1080/00337578308207402.

Sunta, C.M., 1984. A review of thermoluminescence of calcium fluoride, calcium sulphate and calcium carbonate. Radiat. Protect. Dosim. 8 (Issue 1–2), 25–44. https://doi.org/10.1093/oxfordjournals.rpd.a083041, 1 March 1984.

Topaksu, M., Correcher, V., Garcia-Guinea, J., 2016. Luminescence emission of natural fluorite and synthetic CaF_2:Mn (TLD-400). Radiat. Phys. Chem. 119, 151–156.

Trowbridge, J., Burbank, J.E., 1898. Phosphorescence produced by electrification. Am. J. Sci. 5, 25–26. Apud McKeever. SWS. A Course in Luminescence Measurements and Analyses for Radiation Dosimetry. Wiley. 2022.

Trzesniak, P., Yoshimura, E.M., Cruz, M.T., Okuno, E., 1990. Brazilian fluorite-based dosimetric pellets: history and post-use review. Radiat. Protect. Dosim. 34 (Issue 1–4), 167–170. https://doi.org/10.1093/oxfordjournals.rpd.a080874.

Umisedo, N.K., et al., 2020. Development of a mechanically resistant fluorite-based pellet to be used in personal dosimetry. Radiat. Meas. 134, 106330 https://doi.org/10.1016/j.radmeas.2020.106330.

Valerio, M.E.G., Blak, A.R., Chadwick, A.V., 1991. Relaxation processes in calcium fluoride solid solutions with rare-earth and aluminium fluorides Rad. Eff. Defects Solids 119–121. https://doi.org/10.1080/10420159108224907, 393–398.

Williams, O.M., Spooner, N.A., 2020. Quartz optically stimulated luminescence configurational coordinate model. Radiat. Meas. 132, 106259 https://doi.org/10.1016/j.radmeas.2020.106259.